A theoretical study on the isomerization and dissociation kinetics of methyl decanoate radicals

Qinghui Meng[a,b], Yicheng Chi[a], Lidong Zhang[b,*], Peng Zhang[a,*], Liusi Sheng[b]
a. Departmental of Mechanical Engineering, The Hong Kong Polytechnic University, Hung Hom, Kowloon, Hong Kong

b. National Synchrotron Radiation Laboratory, University of Science and Technology of China, Hefei, Anhui, China

1 Introduction

Biodiesel is regarded as one of the most promising fuel alternatives for its renewable and various feedstocks, environmental benefits, and attractive physicochemical properties [1]. Methyl decanoate [MD, $CH_3(CH_2)_8COOCH_3$], has been proposed as a typical biodiesel surrogate. Its desirable fuel properties (e.g. low vapor pressure and melting point) make it experimentally accessible to traditional techniques.

For biodiesel surrogate molecules with heavy atoms more than 10, energy calculations with the forementioned high-level methods are formidable due to their intensive computation load. To meet this challenge, a two-layer ONIOM method was developed by Zhang et al. [2, 3], aiming to directly calculate the accurate thermochemical and chemical kinetic parameters of the practical biodiesel constituents. The method was systematically validated for the H-abstraction reactions of saturated esters $C_nH_{2n+1}COOC_mH_{2m+1}$ (n = 1–5, 9, 15; m = 1, 2) and unsaturated esters $C_nH_{2n-1}COOCH_3$ (n = 2–5, 17) by hydrogen radicals. The predictions for energy barriers and heat of reactions have comparable accuracy with the QCISD(T)/CBS method with deviations being less than 0.15 kcal/mol.

In the present work, the rate constants of the isomerization and dissociation reactions were theoretically investigated for all MD radicals. Density functional theory (DFT) was employed to locate the stationary points on the potential energy surface. Single-point energies were refined with the two-layer ONIOM method of Zhang et al. [2, 3]. Rate constants were then computed with the TST-RRKM theory at temperature from 500K to 2500 K and at the pressures of 0.1, 1, 10 and 100 atm.

2 Theoretical Methodology

The geometry optimizations, vibrational frequencies, and zero-point energies for all of the stationary points on the potential energy surface (PES) of MD radicals were obtained at the M06-2X/6-311++G(d,p) level of theory. The transition states corresponding to desired reaction coordinates were identified by using the imaginary frequencies analysis and visual inspection. For those ambiguous cases, the intrinsic reaction path analysis was utilized to examine the connections of each saddle point to its local minima. All harmonic frequencies used herein are the original data from the density functional theory calculations without using scaling factors [4].

The higher-level single-point energies were calculated by using a two-layer ONIOM method [2, 3], employing the QCISD(T)/CBS for the high layer and the M06-2X-favor DFT method for the low layer. The present ONIOM method predicts the high-level energy of the entire system by its low-level energy plus the correction from the difference between the high-level and low-level energies of the chemically active portion (CAP), given by

$$\mathrm{E^{ONIOM}[High:Low] = E^{Low}(R) + E^{High}(CAP) - E^{Low}(CAP)} \quad \text{(E1)}$$

For the isomerization and dissociation reactions of MD radicals, the CAP consists of the active site and two neighboring CH_2 (or CH_3, COO) groups on the one side and two neighboring CH_2 (or CH_3, COO) groups on the other side. The ONIOM [QCISD(T)/CBS:DFT] energy is calculated by

$$\begin{aligned}\mathrm{E^{ONIOM}[QCISD(T)CBS:DFT]} &= \mathrm{E^{ONIOM}[QCISD(T)/CBS:DFT]_{DZ\rightarrow TZ}} \\ &+ \{\mathrm{E^{ONIOM}[MP2/CBS:DFT]_{TZ\rightarrow QZ}} \\ &- \mathrm{E^{ONIOM}[MP2/CBS:DFT]_{DZ\rightarrow TZ}}\} \end{aligned} \quad \text{(E2)}$$

where

$$\begin{aligned}\mathrm{E^{ONIOM}[QCISD(T)/CBS:DFT]_{DZ\rightarrow TZ}} &= \mathrm{E^{ONIOM}[QCISD(T)/TZ:DFT]} \\ &+ \{\mathrm{E^{ONIOM}[QCISD(T)/TZ:DFT]} \\ &- \mathrm{E^{ONIOM}[QCISD(T)/DZ:DFT]}\} \times 0.4629 \end{aligned} \quad \text{(E3)}$$

$$\begin{aligned}\mathrm{E^{ONIOM}[MP2/CBS:DFT]_{TZ\rightarrow QZ}} &= \mathrm{E^{ONIOM}[MP2/QZ:DFT]} \\ &+ \{\mathrm{E^{ONIOM}[MP2/QZ:DFT]} \\ &- \mathrm{E^{ONIOM}[MP2/TZ:DFT]}\} \times 0.6938 \end{aligned} \quad \text{(E4)}$$

$$\begin{aligned}\mathrm{E^{ONIOM}[MP2/CBS:DFT]_{DZ\rightarrow TZ}} &= \mathrm{E^{ONIOM}[MP2/TZ:DFT]} \\ &+ \{\mathrm{E^{ONIOM}[MP2/TZ:DFT]} \\ &- \mathrm{E^{ONIOM}[MP2/DZ:DFT]}\} \times 0.4629 \end{aligned} \quad \text{(E5)}$$

The ONIOM [QCISD(T)/CBS:DFT] method has been systematically validated in the previous theoretical studies on the H-abstraction reactions of saturated and unsaturated alkyl esters by hydrogen radicals, and its reliability has been confirmed through comparisons with the QCISD(T)/CBS results with deviations being less than 0.15 kcal/mol [2, 3]. ll the present calculations were performed by using the Gaussian 09 program [5].

For the reactions with well-pronounced transition states, the transition state theory (TST) was used for the calculation of rate constants, where the rigid rotor harmonic oscillator (RRHO) assumption was employed for all the internal degrees of freedom except for those low-frequency torsional modes. For each torsional mode, the hindrance potentials as a function of the torsional angle were explicitly obtained at the M06-2X/6-311++G(d,p) level via relaxed potential energy surface scans with a increment angle of 12˚. For the reactions involving the transfer of hydrogen atoms, the tunneling effect on the rate constants was routinely taken into account on base of the asymmetric Eckart model [6].

3 Results and discussions

3.1 Potential energy surfaces

The nomenclature of these ten different radicals is consistent with that used in the previous study[14]. To be specific, the radicals $CH_3(CH_2)_7CHCOOCH_3$, …, $CH_2(CH_2)_8COOCH_3$ and $CH_3(CH_2)_8COOCH_2$ are denoted by MD2J, …, MD10J and MDMJ, respectively. The isomer $CH_3(CH_2)_6CHCH=C(OH)OCH_3$ is denoted by R11.

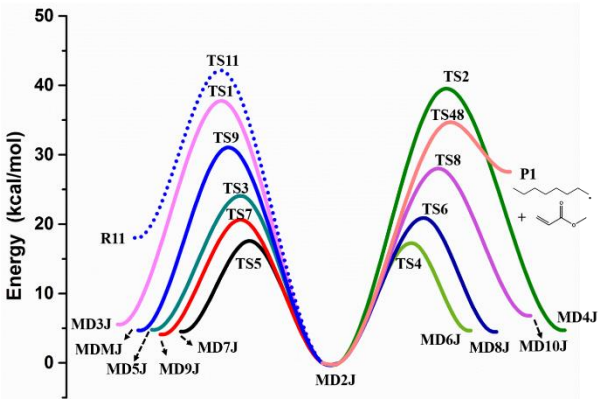

Fig. 1. Potential energy surface for the isomerization and *β*-scission reactions of MD2J at the ONIOM [QCISD(T)/CBS:DFT]//M06-2X/6-311++G(d,p) level.

The PES for MD2J is displayed in Fig. 1, where the *β*-scission reaction forming n-heptane radical and methyl acrylate (i.e. P1) was chosen as the entrance channel. The other *β*-scission reaction leading to $CH_3(CH_2)_7CH=C=O$ and CH_3O has a very high energy barrier compared with the other reactions in the PES and therefore is not shown for clearer illustration. As shown in Fig.1, MD2J can isomerize to MD3J, MD4J, …, MD10J, and MDMJ via hydrogen migration reactions with energy barriers ranging from 17.1 kcal/mol to 39.2 kcal/mol.

3.2 High-pressure rate constants

Scarcely available kinetic parameter of MD makes the direct comparison unfeasible to conduct. Thus, the reactions involving these representative radicals, such as MD2J and MB2J, MDMJ and MBMJ, were chosen respectively to show the difference between their isomerization reactions MD2J→MDMJ and MB2J→MBMJ, as well as that between their *β*-scission reactions MD2J→P1 and MB2J→P. The isomerization reactions MDMJ→MD2J and MBMJ→MB2J, as well as the *β*-scission reactions MDMJ→P16 and MBMJ→P were also shown for comparison.

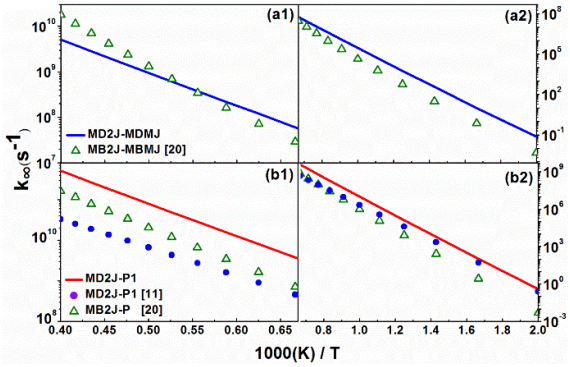

Fig. 2. High-pressure limit rate coefficients for the representative (a) isomerization and (b) dissociation reactions of MD2J. Rate coefficients of relevant reactions for MD [8] and MB [7] are shown for comparison.

Fig. 2 shows the high-pressure limit rate coefficients for the representative (a) isomerization and (b) dissociation reactions of MD2J. Relevant kinetic data of some isomerization and β-scission reactions for MB radicals by Huynh et al. [7] and for MD radicals by Herbinet et al. [8] are also shown for comparison. The temperature range considered in this work was split into two temperature regimes to facilitate the comparison. It is seen that the rate constants of MD2J→MDMJ are close to those of MB2J→MBMJ only in a narrow temperature range around 2000K. The one-order-of-magnitude difference of rate constants between MD2J→MDMJ and MB2J→MBMJ is observed at temperature less than 800K, due to their energy difference. At low temperatures, the rate constants of MB2J→P are lower than those of MD2J→P1, whereas the rate constants of MD2J→P1 obtained by Herbinet et al. [8] agree well with the present results.

3.3 Pressure-dependent rate constants

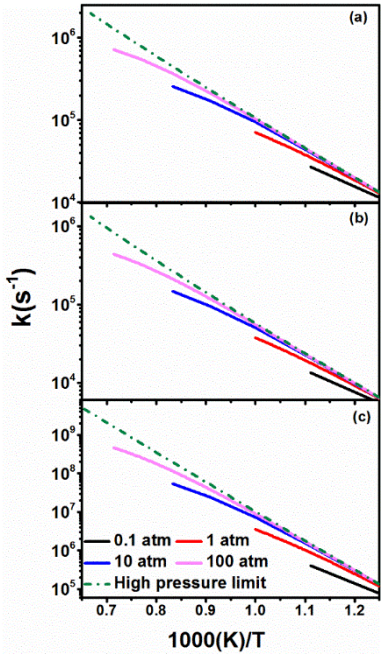

Fig. 3. The temperature and pressure-dependent rate coefficients for kinetically favorable reactions of MD2J. (a) MD2J-MD6J, (b) MD2J-MD7J, (c) MD2J-P1.

The pressure-dependent rate constants for three representative reactions of MD2J are illustrated in Fig. 3, where the pressure-dependent rate plots at intermediate and high temperatures have been zoomed in to manifest their difference. It is seen that the pressure-dependent rate plots end at certain temperatures due to the "well merging" phenomena in the reaction system [9]. At sufficiently high temperatures, it is common for some of the radical isomers (i.e. potential wells) to rapidly equilibrate with each other or with bimolecular products. Consequently, beyond the temperature at which the well merging occurs, the merged wells become chemically indistinguishable and should be considered as a "combined" well, and the total number of wells in the PES is accordingly reduced by one. In the present work, the well-reduction based on the multi-well master equation analysis will not be discussed in detail, and a recently developed method that automates this reduction process has been incorporated into the MESS computer code [10].

Regarding the pressure dependence of the rate constants at all pressures considered in this work, the branching ratios of reactions from the MD2J at 0.1 atm, 1 atm, 10 atm and 100 atm are shown in Fig. 4. Although branching ratios of main isomerization reactions decline rapidly with the temperature increases, they are the predominant consumption at low temperatures. In contrast, the branching ratio of the β-scission (MD2J→P1) has a rapid growth and reaches approximate equilibrium at sufficiently high temperatures. Therefore, the distribution of MD radicals depends on not only the initial steps but also the isomerization reactions, which may affect the autoignition properties of MD.

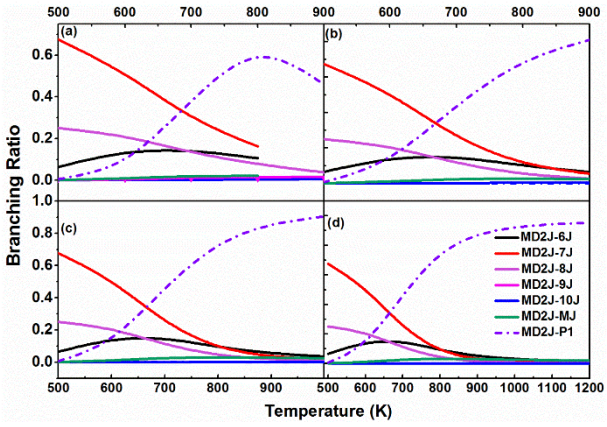

Fig. 4. Temperature-dependent branching ratios for main reactions of MD2J at (a) 0.1atm, (b)1atm, (c)10atm, and (d)100 atm.

4 Conclusions

In the present theoretical study, the rate constants of the isomerization and dissociation reactions for methyl decanoate radicals were calculated by using the transition state theory. Phenomenological rate constants of the isomerization and dissociation reactions of methyl decanoate radicals were obtained by the RRKM/ME theory. At intermediate temperatures, intense competitions between isomerization and dissociation reactions, determining the distribution of MD radicals, are of great significance to the autoignition. At temperature higher than 1100K, the chemical kinetics of MD radicals is well described by the dissociation

via β-scissions. Moreover, the significant pressure dependence of rate constants was observed for isomerization and dissociation reactions of MD radicals.

Compared with the available literature data of MB, n-decane, and MD, great discrepancies between MB and MD have been found for the reactions specific to methyl esters. The present results suggest that kinetic parameters used in MD modeling by analogy to corresponding alkanes have significant errors for isomerization reactions, whereas they are approximately suitable for simulating the β-scission reactions of MD because of their comparable energy barriers.

Acknowledgements

The work at the Hong Kong Polytechnic University was supported by NSFC (No. 91641105), and partly by the university matching grant (4-BCE8). The work at University of Science and Technology of China was supported by, Natural Science Foundation of China (51676176, U1532137, 11575178 and 21373193), National Key Scientific Instruments and Equipment Development Program of China (2012YQ22011305)，and Fundamental Research Funds for the Central Universities (WK2320000038).

References:

[1] Agarwal A.K., (2007).Biofuels (alcohols and biodiesel) applications as fuels for internal combustion engines. Prog. Energy Combust. Sci. 233-271.

[2] Zhang L., P. Zhang, (2015).Towards high-level theoretical studies of large biodiesel molecules: an ONIOM [QCISD(T)/CBS:DFT] study of hydrogen abstraction reactions of C(n)H(2n+1)COOC(m)H(2m+1) + H. Phys. Chem. Chem. Phys. 200-208.

[3] Zhang L., Q. Meng, Y. Chi, P. Zhang, (2018).Toward High-Level Theoretical Studies of Large Biodiesel Molecules: An ONIOM [QCISD(T)/CBS:DFT] Study of the Reactions between Unsaturated Methyl Esters (CnH2n–1COOCH3) and Hydrogen Radical. J. Phys. Chem. A. 4882-4893.

[4] Zhang P., S.J. Klippenstein, C.K. Law, (2013).Ab initio kinetics for the decomposition of hydroxybutyl and butoxy radicals of n-butanol. J. Phys. Chem. A. 1890-1906.

[5] Frisch M., G. Trucks, H.B. Schlegel, G. Scuseria, M. Robb, J. Cheeseman, G. Scalmani, V. Barone, B. Mennucci, G. Petersson, (2009).Gaussian 09, revision a. 02, gaussian. Inc., Wallingford, CT.

[6] Eckart C., (1930).The penetration of a potential barrier by electrons. Phys. Rev. 1303.

[7] Huynh L.K., A. Violi, (2008).Thermal decomposition of methyl butanoate: Ab initio study of a biodiesel fuel surrogate. J. Org. Chem. 94-101.

[8] Herbinet O., W.J. Pitz, C.K. Westbrook, (2010).Detailed chemical kinetic mechanism for the oxidation of biodiesel fuels blend surrogate. Combust. Flame. 893-908.

[9] Klippenstein S.J., J.A. Miller, (2002).From the Time-Dependent, Multiple-Well Master Equation to Phenomenological Rate Coefficients. J. Phys. Chem. A. 9267-9277.

[10] Georgievskii Y., J.A. Miller, M.P. Burke, S.J. Klippenstein, (2013).Reformulation and solution of the master equation for multiple-well chemical reactions. J. Phys. Chem. A. 12146-12154.